Effect of Temperature on Photovoltaic Solar Energy Conversion*

JOSEPH J. WYSOCKI AND PAUL RAPPAPORT
RCA Laboratories, Princeton, New Jersey

(Received August 3, 1959)

Photovoltaic solar energy conversion is investigated theoretically over a temperature range of 0–400°C using semiconductor materials with band gaps varying from 0.7 to 2.4 ev. Three cases are considered. In Case *I*, the junction current is the ideal current. In Case *II*, the junction current is the ideal plus a recombination current; and in Case *III*, a recombination current. The best conversion performance is obtained for the ideal current; the worst, for the recombination current. The maximum conversion efficiency occurs in materials with higher band gap as the temperature is increased. GaAs is close to the optimum material for temperatures below 200°C. Experimental measurements are presented on Si, GaAs, and CdS cells. The measurements on Si and GaAs agree with theoretical expectations as far as the gross behavior is concerned. The CdS cell behaves anomalously as if it were made from a material with band gap of 1.1 ev.

TABLE OF SYMBOLS

a	concentration gradient in a diffused junction
α	absorption coefficient in a semiconductor
D_n	diffusion constant for electrons
D_p	diffusion constant for holes
D	$D_n[1+(D_p/D_n)^{\frac{1}{2}}]^2$, effective diffusion constant
E_g	energy gap of a semiconductor
E_f	Fermi energy level
E_T	energy level of traps
E_i	intrinsic energy level
ϵ	permittivity of semiconductor
g	generation rate of electron-hole pairs per cm^3 per sec
I_s	short-circuit current density
I_j	junction current density
I_L	load current density
I_{mp}	load current density at maximum power
I_0	reverse saturation current of a *p-n* junction
k	Boltzmann's constant
κ	dielectric constant of semiconductor
L_n	diffusion length of electrons
L_p	diffusion length of holes
l	thickness of absorbing semiconductor
m_p^+	hole effective mass for density of states
m_n^+	electron effective mass for density of states
$n_{ph}(E_G)$	number of photons with energy greater than the band gap E_G
η	solar conversion efficiency
N_A	number of net acceptor impurities per unit volume
N_D	number of net donor impurities per unit volume
N_s	geometrical mean of the number of states in the conduction and valence bands
n_i	intrinsic carrier density
ϕ	barrier height in a *p-n* junction
P_{mp}	maximum power output of a solar converter
Q	collection efficiency of *p-n* junction
R_{mp}	load resistance at maximum power
r	reflection coefficient of front face of solar converter
T	temperature in °K
τ_n	electron lifetime
τ_p	hole lifetime
τ_{no}	electron lifetime in material in which all the traps are empty
τ_{po}	hole lifetime in material in which all the traps are full
V_{mp}	voltage at maximum power
W	width of the depletion region
λ	q/kT

INTRODUCTION

A SEMICONDUCTOR photovoltaic cell converts solar energy directly into electrical energy by means of a *p-n* junction. Incident photons with energies greater than the band gap of the semiconductor create electrons and holes which are separated by the junction. A potential is thus created across the junction, and energy can be delivered to a resistive load.[1–12] The factors which make the conversion process temperature dependent are introduced by the properties of the semiconductor and the behavior of *p-n* junctions. This temperature dependence is the subject of the present paper. The discussion will be concerned with solar energy conversion. However, the conclusions are equally applicable to the conversion of other forms of ionizing radiation.

* This work was supported by the U. S. Army Signal Research and Development Laboratory, Fort Monmouth, New Jersey.

[1] Early history: V. K. Zworykin and E. G. Ramberg, *Photoelectricity and Its Applications* (John Wiley & Sons, Inc., New York, 1949).
[2] K. Lehovec, Phys. Rev. **74**, 463 (1948).
[3] R. Cummerow, Phys. Rev. **95**, 16 (1954).
[4] R. Cummerow, Phys. Rev. **95**, 561 (1954).
[5] Reynolds, Leies, Antes, and Marburger, Phys. Rev. **96**, 533 (1954).
[6] E. Rittner, Phys. Rev. **96**, 1708 (1954).
[7] Chapin, Fuller, and Pearson, J. Appl. Phys. **25**, 676 (1954).
[8] W. Pfann and W. van Roosbroeck, J. Appl. Phys. **25**, 1422 (1954).
[9] M. Prince, J. Appl. Phys. **26**, 534 (1955).
[10] Jenny, Loferski, and Rappaport, Phys. Rev. **101**, 1208 (1956).
[11] J. J. Loferski, J. Appl. Phys. **27**, 777 (1956).
[12] Rappaport, Loferski, and Linder, RCA Rev. **17**, 100 (1956).

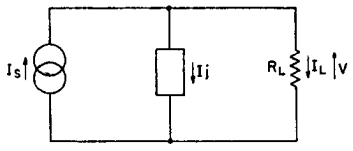

(1) $I_L = I_S - I_j$

(2) $I_j = \Sigma I_0(e^{\lambda V} - 1)$

FIG. 1. Equivalent circuit of photovoltaic solar converter.

THEORY

1. General

The equivalent circuit of a photovoltaic cell[11,12] is shown in Fig. 1. Series resistances and shunt conductances are assumed negligible.

The junction current I_j is related to the junction voltage V by an equation of the form,

$$I_j = \sum I_0(e^{\lambda V} - 1) \tag{1}$$

where the summation sign is used to indicate that more than one mechanism may determine the junction behavior; i.e., the total current may be the sum of the ideal junction current,[13] a recombination current,[14] and a leakage current,[15] all of which can have a voltage dependence of the type shown under certain conditions. The short-circuit current I_s is related to the input radiation by the following equation[11]

$$I_s = Q(1-r)(1-e^{-\alpha l})qn_{ph}(Eg). \tag{2}$$

When the p-n junction is suitably located and the lifetimes are sufficiently great, I_s can be express as[16]

$$I_s = qg[L_n + L_p]. \tag{3}$$

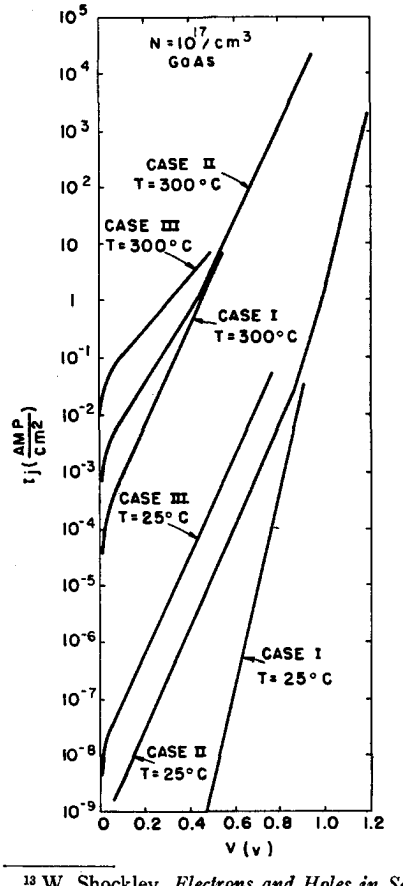

FIG. 2. Junction current *vs* voltage.

2. Effect of Temperature on I_s

The temperature dependence of the short-circuit current arises primarily with the diffusion lengths, which can be expressed as

$$L = (D\tau)^{\frac{1}{2}}. \tag{4}$$

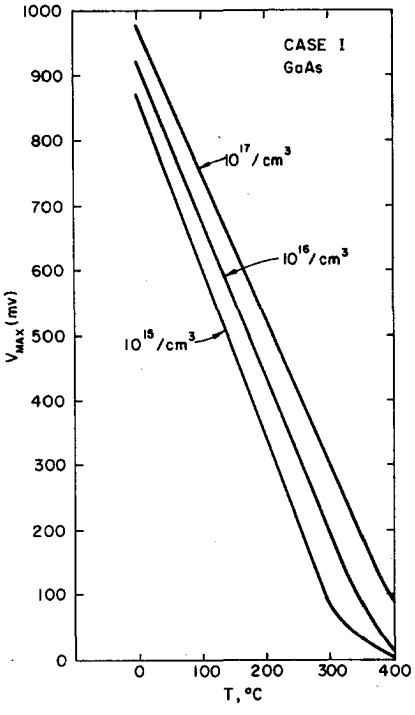

FIG. 3. V_{max} *vs* T, N as parameter.

Since the temperature dependence of the diffusion constant is $T^{-\frac{1}{2}}$, the net effect on L is small. It was assumed that the temperature dependence of the lifetime is determined by the single-level recombination statistics of Hall, Shockley, and Read[17,18] who show the lifetime in the n-type region to be

$$\tau = \tau_{po}\left[1 + \exp\left(\frac{E_T - E_F}{kT}\right)\right], \tag{5}$$

and

$$\tau = \tau_{no} + \tau_{po}\exp\left(\frac{E_T + E_F - 2E_i}{kT}\right) \tag{6}$$

[13] W. Shockley, *Electrons and Holes in Semiconductors* (D. Van Nostrand Company, Inc., Princeton, New Jersey, 1950), p. 314.
[14] Sah, Noyce, and Shockley, Proc. Inst. Radio Engrs. **45**, 1228 (1957).
[15] M. Cutler and H. Bath, Proc. Inst. Radio Engrs. **45**, 39 (1957).
[16] R. Gremmelmaier, Proc. Inst. Radio Engrs. **46**, 1045 (1958).
[17] W. Shockley and W. T. Read, Phys. Rev. **87**, 835 (1952).
[18] R. Hall, Phys. Rev. **87**, 387 (1952).

in the p-type region. The temperature dependence of the lifetime arises from the exponential terms in the foregoing equations. If the difference between E_F and E_T is large compared to kT, the exponential terms in Eq. (5) and (6) are negligible, and they remain negligible as the temperature is increased until E_F is within a few kT of E_T. The temperature at which the lifetime increases depends upon the doping and the trap level. For convenience in performing the calculations, the trap level will be located at the intrinsic Fermi level. The lifetime will thus be approximately constant in the temperature range in which solar energy conversion will be considered for material with a doping level of 10^{17} per cm^3.

Another factor in I_s to consider is the generation rate g. The generation rate increases slightly with temperature. This increase is due to the decrease in band gap, and consequent increase in the number of photons which are effective in creating electron-hole pairs. The effect is small in the temperature range considered, however, and will be neglected.

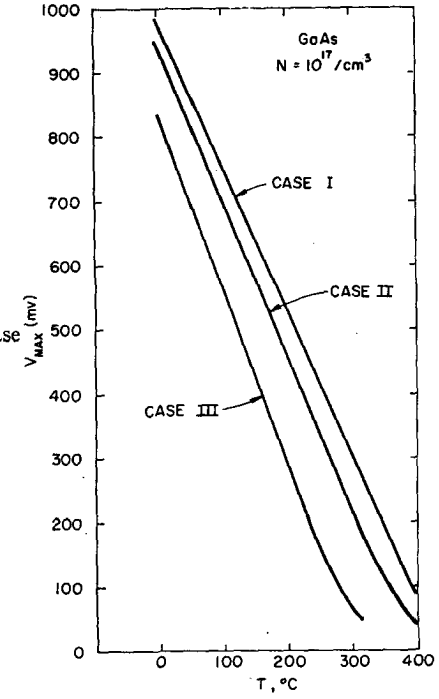

FIG. 4. V_{max} *vs* T, case as parameter.

It is concluded that I_s is not a rapidly varying function of T for heavily doped material, and its temperature dependence will be neglected hereafter.

3. Effect of Temperature on I_j

The junction current, as has been indicated, can be determined by several mechanisms. The leakage mechanism will not be considered in what follows because leakage through surface channels gives rise to equations similar in form to those obtained with the recombination model. Its effect can be inferred, therefore, from the results obtained with the recombination model. The following two mechanisms will be considered in detail.

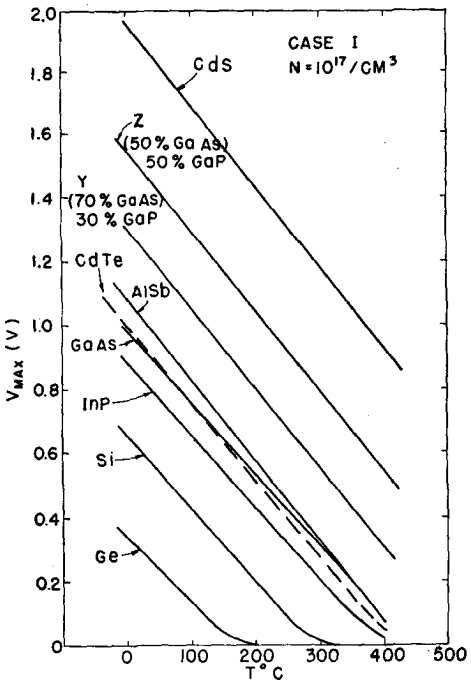

FIG. 5. V_{max} *vs* temperature.

a. Ideal Junction Current

This current arises from carriers which flow over the junction barrier; it depends upon voltage in the follow-

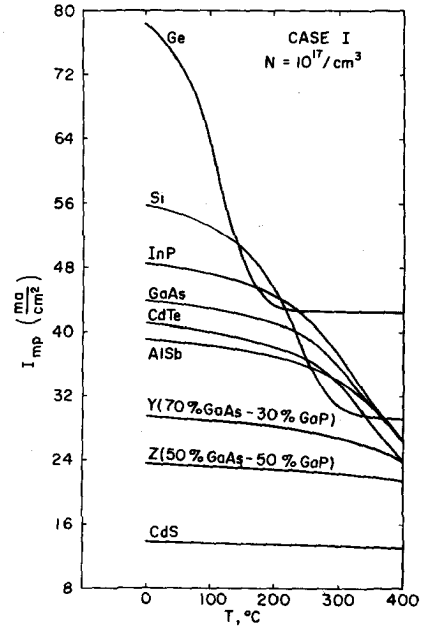

FIG. 6. I_{mp} *vs* temperature.

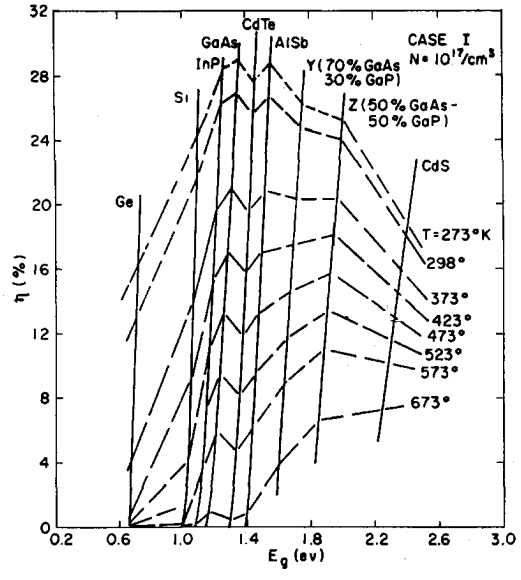

FIG. 7. Efficiency *vs* energy gap.

ing manner[13]:

$$I_j = I_0\left[\exp\left(\frac{qV}{kT}\right)-1\right], \tag{7}$$

$$I_0 = qn_i^2\left[\frac{1}{N_A}\left(\frac{D_n}{\tau_n}\right)^{\frac{1}{2}}+\frac{1}{N_D}\left(\frac{D_p}{\tau_p}\right)^{\frac{1}{2}}\right]. \tag{8}$$

The behavior predicted by Eqs. (7) and (8) is well known. The magnitude of I_0 and I_j is determined primarily by the band gap of the semiconductor through its effect on the square of the intrinsic density n_i^2. The coefficient I_0 increases exponentially with temperature resulting in an exponential increase in I_j.

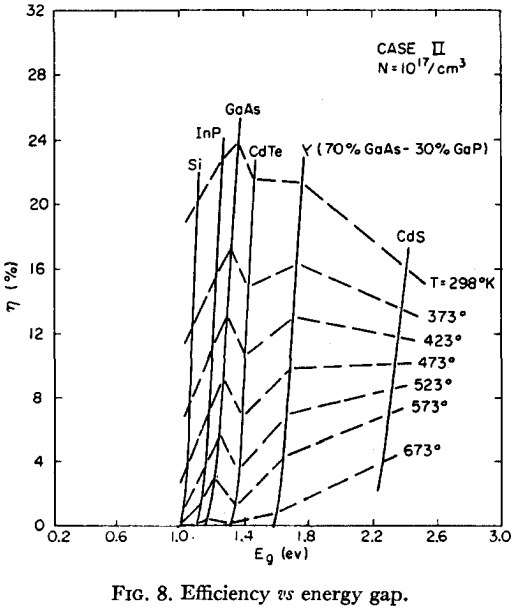

FIG. 8. Efficiency *vs* energy gap.

b. Recombination current

The recombination current arises from carriers which recombine in the depletion region from centers existing in the forbidden gap.[14] For single-level centers, the current is determined by integrating the Shockley-Read expression for the recombination rate[17] over the depletion region, leading to the following equation[14]:

$$I_j = \frac{qn_i}{(\tau_{p0}\tau_{n0})^{\frac{1}{2}}} W \frac{2\sinh(qV/2kT) f(b)}{(\phi - V)(q/kT)}. \tag{9}$$

$f(b)$ is a slowly varying function of the voltage, trap level, lifetimes, and barrier height. The magnitude of the current varies as n_i, instead of n_i^2 consequently, it is determined by half the band gap. The current increases exponentially with temperature with an activation energy which depends upon the location of the trap level.

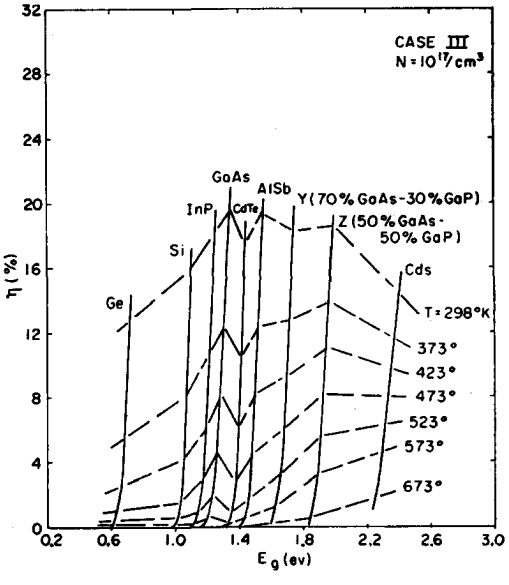

FIG. 9. Efficiency *vs* energy gap.

4. Effect of Temperature on Solar Energy Conversion

The temperature effects already considered were incorporated into the equations governing photovoltaic energy conversion, and conversion performance was calculated as a function of temperature. The calculations were performed on an IBM 650 Digital Computer. Three cases were considered.

In Case *I*, I_j was the ideal junction current. Consequently the equations for photovoltaic energy conversion could be put into the following closed form:

$$V_{\max} = \ln\left(\frac{I_s}{I_0}+1\right), \tag{10}$$

TABLE I. Semiconductor parameters used in calculations. (Note: estimated and state-of-the-art values.)

Semiconductor	μ_n cm²/v-sec	μ_p cm²/v-sec	$\tau_p = \tau_n$ (sec)	m_n^+	m_p^+	n_i No./cm³ (300°K)	κ	I_s (ma/cm²)	E_g (ev)
Ge	3000	1350	10^{-6}	0.55	0.36	8.3×10^{12}	16	85	$0.83-4\times10^{-4}\,T$
Si	710	360	10^{-7}	1.08	0.60	1.1×10^{10}	12	58	$1.2-3.5\times10^{-4}\,T$
InP	4000	100	10^{-8}	0.08	0.60	8×10^{7}	11	50	$1.39-4.6\times10^{-4}\,T$
GaAs	5000	400	10^{-8}	0.06	0.50	9.2×10^{6}	11	45	$1.5-5\times10^{-4}\,T$
CdTe	300	30	10^{-8}	1.08	0.60	1.2×10^{7}	12	42	$1.57-4\times10^{-4}\,T$
AlSb	710	360	10^{-8}	1.08	0.60	1.7×10^{6}	10	40	$1.67-4\times10^{-4}\,T$
Y (70% GaAs–30% GaP)	200	20	10^{-8}	1.08	0.60	3.7×10^{4}	12	30	$1.9-4\times10^{-4}\,T$
Z (50% GaAs–50% GaP)	200	20	10^{-8}	1.08	0.60	3.1×10^{2}	12	24	$2.1-4\times10^{-4}\,T$
CdS	200	20	10^{-8}	1.08	0.60	1.2×10^{-1}	12	14	$2.52-4\times10^{-4}\,T$

$$R_{mp}=\frac{1}{\lambda I_0 e^{\lambda V_{mp}}}, \tag{11}$$

$$e^{\lambda V_{mp}}(1+\lambda V_{mp})=\frac{Is}{I_0}+1, \tag{12}$$

$$I_{mp}=\lambda V_{mp} e^{\lambda V_{mp}} I_0, \tag{13}$$

$$\eta=\frac{\lambda V_{mp}^2}{1+\lambda V_{mp}}\frac{I_s}{1.35}\left(1+\frac{I_0}{I_s}\right), \tag{14}$$

for a power input of 135 mw/cm². I_0 is given by Eq. (8).

The junction current in Case *II* was the sum of the ideal junction current and a recombination current.

$$I_j=I_0(e^{\lambda V}-1)+I_n\frac{\sinh(\lambda V/2)}{\lambda(\phi-V)}f(b), \tag{15}$$

where

$$f(b)=\int_{z_1}^{z_2}\frac{dz}{Z^2+2bZ+1}; \tag{16}$$

$$b=\exp\left(-\frac{\lambda V}{2}\right); \tag{17}$$

$$Z_{1,2}=e^{\mp\lambda/2(\phi-V)}; \tag{18}$$

and

$$I_n=\frac{2qn_i}{(\tau_{p0}\tau_{n0})^{\frac{1}{2}}}[(12\epsilon/qa)(\phi-V)]^{\frac{1}{2}}. \tag{19}$$

I_0 is again given by Eq. (8). The energy conversion equation could not be put into closed form for this case.

In Case *III*, I_j was a recombination current given by

$$I=I_n'\left[\exp\left(\frac{\lambda V}{2}\right)-1\right], \tag{20}$$

with

$$I_n'=\frac{qn_i}{(\tau_{po}\tau_{no})^{\frac{1}{2}}}[(12\epsilon/qa)\phi]^{\frac{1}{2}}. \tag{21}$$

The energy conversion equations could again be put into closed form yielding equations similar to Eqs. (10)–(14) with the exceptions that I_0 is replaced by I_n' and λ is divided by 2.

5. Assumptions and Values Used in Calculations

Semiconductors with band gaps ranging from 0.7 to 2.4 ev were studied over a temperature range of 0–400°C. The generated current I_s was determined by solar conditions outside the atmosphere where the solar power density is 135 mw/cm². The number of photons

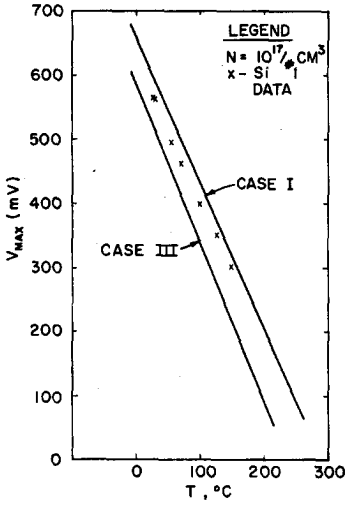

FIG. 10. V_{max} *vs* temperature—silicon solar cell.

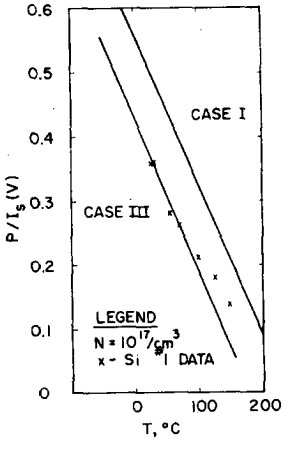

FIG. 11. P/I_s *vs* temperature for silicon solar cell.

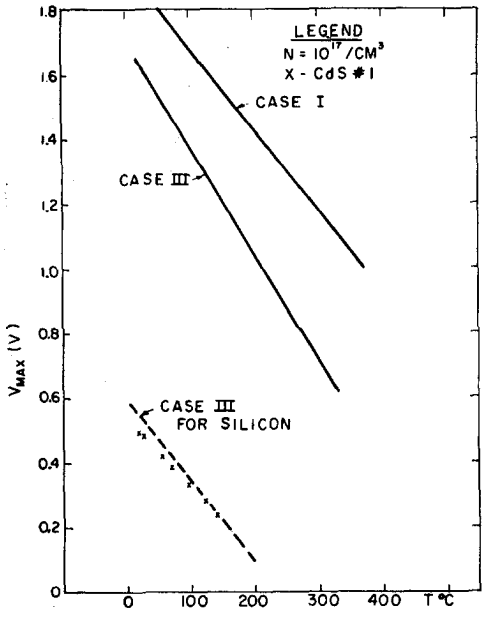

FIG. 12. V_{max} *vs* temperature for cadmium sulfide.

effective in creating hole-electron pairs was taken from published curves.

The following assumptions were made to simplify and to facilitate the calculations. The collection efficiency was taken as unity. Losses due to reflection, leakage conductance, and series resistance were assumed negligible. The electron and hole lifetimes, and impurity concentrations in the n and p regions were assumed equal. Traps were located at the intrinsic energy level and a concentration gradient of 4×10^{19} per cm^4 was assumed for diffused junctions.

Table I lists the values used in the calculations for the various semiconductor parameters. These values are state-of-the-art values in some cases, and in others estimates of the actual values.

RESULTS

The results of the calculations are summarized in Figs. 2 through 10. Figure 2 illustrates the forward current-voltage characteristic of a GaAs p-n junction for the different cases assumed in the calculations. Two sets of curves are shown—one for a temperature of 25°C and the other for 300°C.

Figure 3 shows V_{max} of a GaAs solar converter as a function of doping for Case I. The curves indicate that the highest value of V_{max} and the lowest rate of decrease with temperature is obtained at the higher doping levels. The effect of the different I_j on V_{max} of a GaAs junction doped to 10^{17} per cm^3 is depicted in Fig. 4. It is obvious that best performance is obtained with Case I operation. Figure 5 is a plot of V_{max} *vs* T for the semiconductors investigated for Case I and a doping level of 10^{17} per cm^3. The slopes of the lines are all roughly the same—approximately 2 mv/°C. The maximum voltage is greater, of course, for higher band gap values.

A composite curve of I_{mp} *vs* T for Case I and a doping level of 10^{17} per cm^3 is shown in Fig. 6. I_{mp} approaches $\frac{1}{2}I_s$ as the temperature is increased. This asymptotic behavior is a consequence of the fact that junction resistance approaches zero as the temperature is increased. It is therefore not apparent in the higher band gap materials over the temperature range studied.

Composite curves of efficiency and power *vs* bandgap are shown in Figs. 7 to 9. Case I is considered in Fig. 7.

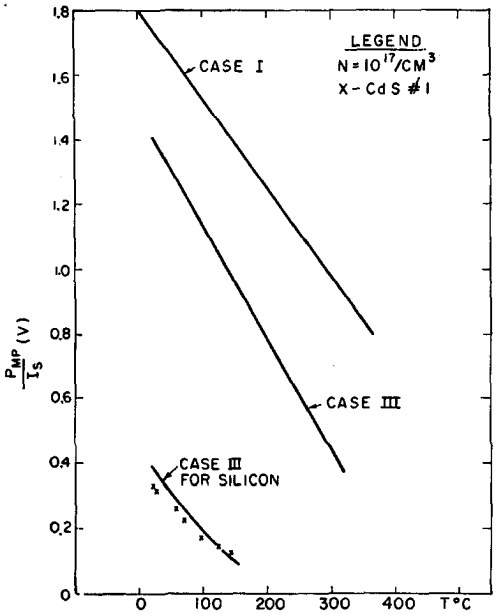

FIG. 13. P_{mp}/I_s *vs* temperature for cadmium sulfide.

The material with optimum efficiency at room temperature is GaAs.[11] The optimum shifts to higher bandgaps as the temperature is increased in agreement with the results of Halsted.[19]

Figure 8 shows the efficiency for Case *II*, while Fig. 9 is a similar plot for Case *III*. The optimum band gap is roughly the same for all cases, however the efficiency is much less for Case *III* as compared to Case *I*.

TABLE II. Characteristics of Cells.

Cell	Area (cm²)	Room temperature efficiency
Silicon	1.7	10%
GaAs	0.2	3.8
CdS	0.385	3.6

COMPARISON WITH EXPERIMENT

Measurements were made on three cells. Table II specifies the area and room temperature efficiency of each cell. The silicon cell was a commercial unit made by Hoffman Semiconductor Corporation and the CdS cell was kindly furnished by Reynolds of WADC.

[19] R. Halsted, J. Appl. Phys. 28, 1131 (1957).

During measurement, the cells were mounted in a small furnace with a glass window to allow the cells to be irradiated. A Chromel-Alumel thermocouple was attached to the cells to measure the temperature, and dry helium was pumped through the system to maintain a standard atmosphere. A light source supplied an input power density of 100 mw/cm² to the cells.

The results of the measurements are plotted in Figs. 10 to 16 together with theoretical curves for Case *I* and Case *III* at a doping level of 10^{17} per cm³. Figure 10 is a plot of V_{max} *vs* T for silicon. The experimental points fall between the theoretical curves, and the rate of decrease agrees well with the theoretical value. Similar agreement is found in Fig. 11 where (P_{mp}/I_s) is plotted *vs* T.

The CdS curves are shown in Figs. 12 and 13. The experimental points fall below the theoretical curves; in fact, they lie roughly on the theoretical curves for Si, Case *III*.

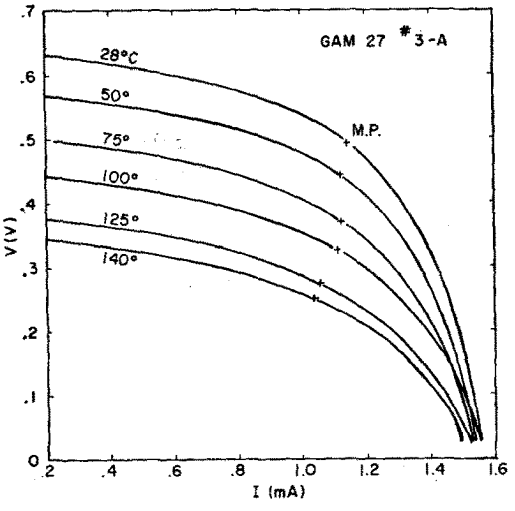

FIG. 14. Current-voltage characteristics of gallium arsenide cell *vs* temperature.

The curves for GaAs are shown in Figs. 14 to 16. Figure 14 is a plot of the *i–v* characteristics of the GaAs cell in the light with temperature as a parameter. The figure illustrates that I_s is substantially independent of T as assumed in the calculations. The experimental curves in Figs. 15 and 16 are somewhat below the theoretical curves but not to as great an extent as in the case of CdS. The theoretical curves for Si, Case *III*, are also shown for comparison.

The temperature measurements on these cells agree quite well with theory as far as the rates of decrease with temperature is concerned. The lack of agreement in absolute values in some cases can be ascribed to the use of nonoptimum cells. One feature of the measurements is the behavior of the CdS cell which corroborates the results found in spectral analyses of similar cells where appreciable absorption is found at wavelengths

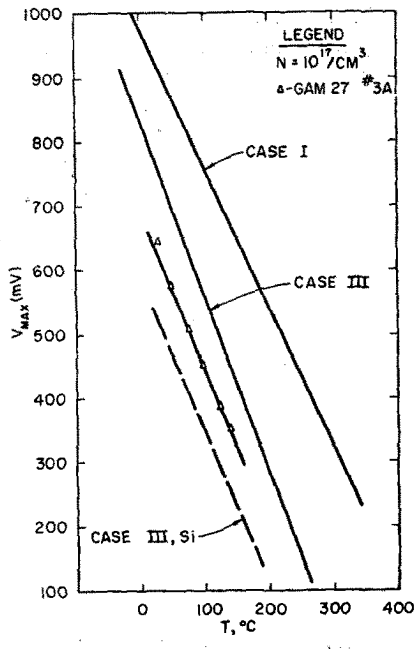

FIG. 15. Maximum voltage *vs* temperature for gallium arsenide solar cell.

greater than that corresponding to the band edge.[20] The spectral response and the temperature behavior of the solar cell indicate that the CdS cell is behaving as if it were made from a material whose band gap is closer to that of Si than that of CdS.

CONCLUSIONS

The optimum conversion performance is obtained when the junction current is the ideal current. A deg-

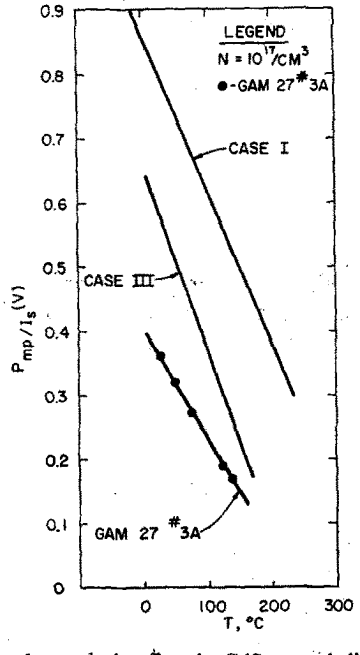

FIG. 16. P_{mp}/I_s *vs* temperature for GaAs solar cell.

[20] D. C. Reynolds, "The photovoltaic effect in CdS crystals," Trans. Conf. Use of Solar Energy (Tucson, Arizona, 1955).

radation in performance results when the current is influenced by recombination or leakage through surface channels. The conversion performance of any given semiconductor improves as the doping level is increased. Practical limits may be set by the onset of degeneracy.

The optimum material for solar energy conversion is a function of temperature. As the temperature is increased, the maximum efficiency shifts to materials with a larger band gap. For temperatures below 200°C, the band gap of GaAs is close to the optimum band gap.

Temperature measurements on a commercial Si cell agree well with theory. Measurements on experimental GaAs and CdS cells indicate the following. The GaAs cell was not optimum. Losses which were not considered in the analysis led to lower values of V_{max} and P_{mp}/I_s than expected. The CdS cell, on the other hand, behaved as if it were made from a material with lower band gap.

ACKNOWLEDGMENTS

The authors wish to acknowledge the suggestions and discussions of Joseph J. Loferski. The calculations were performed by Paul Rygg and Sherwood Skillman.

JOURNAL OF APPLIED PHYSICS VOLUME 31, NUMBER 3 MARCH, 1960

Penetration of Rotating Shaped Charges

SAMPOORAN SINGH
Defence Science Laboratory, Ministry of Defence, New Delhi, India
(Received September 10, 1959)

This paper presents an attempt to correlate theoretically the depth of penetration and the angular velocity of the liner in a rotating shaped charge. Each element of the rotating liner imparts an angular velocity to the corresponding jet element, and this results in a continuous increase of the cross-sectional area of the jet element as it travels in space and a corresponding decrease in the depth of penetration. In order to check the theory, numerical evaluations have been carried out in case of standard M9A1 steel cones. The theoretical results seem to explain the scanty published experimental data of the rotating shaped charges.

IT is well established that when a shaped charge rotates about its axis, there is loss of penetration. Kerr cell photographs[1] and x-ray flash photographs[2] of rotating shaped charges about their axes show that rotation brings about an increase of the cross-sectional area of the jet. The theory of penetration by rotating shaped charges was developed by Singh[3–5] and the basic equation of the theory is

$$\Delta P=\epsilon\Delta L\left(\frac{\gamma\rho}{\rho_t}\right)^{\frac{1}{2}}\left[1-\frac{\sigma}{\rho_t V^2}\left\{\left(\frac{\rho_t}{\gamma\rho}\right)^{\frac{1}{2}}+1\right\}^2\right], \quad (1)$$

where ΔP is the depth penetration, ϵ an empirical constant, ΔL the length of a jet element at the instant when it strikes a target, ρ the density of the liner material, ρ_t the density of the target material, V the mean velocity of the jet element, and the quantity σ is the difference between two quantities, σ_t and σ_j, which represent the resistance of the target and the jet, respectively, to the plastic deformation required by the penetration process. The term γ takes into consideration all corrections for discontinuities within the jet element, i.e. the breakup of the jet into particles and the waver of the jet element due to imperfections in charge or liner; and is given by the expression

$$\gamma=\frac{C\Delta L'}{\Delta L}\left(\frac{R_j}{R_t}\right)^2 \quad (2)$$

and

$$R_t=R_j+S_d\tan\phi+R_r, \quad (3)$$

where $\Delta L'$ represents the length of an element of the jet that is just formed from a finite element in the slant surface of the liner, C an "elongation" constant, R_j the

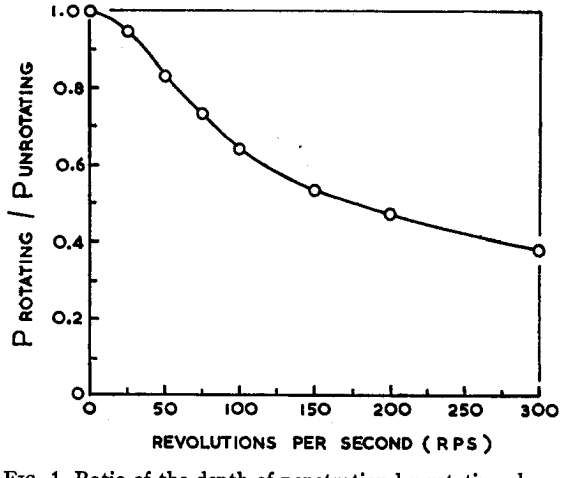

FIG. 1. Ratio of the depth of penetration by rotating charges/depth of penetration by unrotating charges at 7.62 cm standoff distance in mild steel targets as a function of the speed of rotation of the standard M9A1 steel linear in the standard C.I.T. laboratory charge.

[1] L. E. Simon, *German Research in World War II* (John Wiley & Sons, Inc., New York, 1947), p. 119.
[2] R. Schall and G. Thomer, Proceedings of the Second International Congress on High-Speed Photography (Dunod, Paris, 1954).
[3] S. Singh, Proc. Natl. Inst. Sci. India **19**, 665 (1953).
[4] S. Singh, J. Sci. Ind. Research (India) **14B**, 669 (1955).
[5] S. Singh, Proc. Phys. Soc. (London) **71**, 508 (1958).